Interconnect Electromagnetic Modeling using Conduction Modes as Global Basis Functions

Luca Daniel, Alberto Sangiovanni-Vincentelli, and Jacob White

Abstract

A new method is formulated for modeling current distributions inside conductors for a quasi-static or a full-wave electromagnetic field simulator. In our method, we model current distributions inside interconnects using a small number of conduction modes as global basis functions for the discretization of the Mixed Potential Integral Equation. A very simple example is presented to illustrate the potential of our method.

I. Introduction

The past decade's intense development of accelerated integral equation solvers has made it possible to perform electromagnetic analysis of packages or circuit boards with hundreds of conductors in just a few minutes on a workstation [1], [2], [3], [4]. The computational performance provided by these fast algorithms makes it now feasible to consider developing tools which can readily perform full-board analysis, for use in applications such as electromagnetic compatibility diagnosis and resolution. If the application requires many full-wave analyses of entire printed circuit boards, reducing computation time will remain critical, and therefore minimizing the number of unknowns used for each conductor remains an important problem.

The most common approach to minimizing the number of unknowns used to discretize printed circuit board wires is to make a thin conductor, or $2\frac{1}{2}$-d, approximation or a "skin-depth" approximation [5] using surface impedances. In addition, it has been recognized that the many conductor interiors can be decoupled into separate Helmholtz problems which can then be combined with a global exterior Helmholtz problem [6], [7]. The many Helmholtz equations can then be solved either by integral or by differential methods. In this paper we take a somewhat different approach, and make use of the interior Helmholtz equation to generate basis functions for a Galerkin-type solution of the Mixed Potential Integral Equation (MPIE).

The paper is organized as follows: In Section II we summarize the classical integral equation method. In Section III-A, we derive possible "conduction modes" from the solution of the internal electric field Helmholtz equation. Based on such modes, we define in Section III-B global basis functions, that we use in Section III-C for the discretization of the MPIE. Finally, in Section IV a very simple example is used to illustrate the computational attractiveness of our method.

II. Background

For a system of conductors embedded in a medium with constant dielectric permittivity ε, and magnetic permeability μ, the conductor current distribution, $\mathbf{J}$, and the conductor surface charge, ρ, can be determined without computing any fields exterior to the conductors. In particular, the conductor currents can be related to the gradient of a scalar potential, ϕ, using the Mixed Potential Integral Equation (MPIE)

$$\frac{\mathbf{J}(\mathbf{r})}{\sigma} + j\omega\frac{\mu}{4\pi}\int_V \mathbf{J}(\mathbf{r}')\frac{e^{jk_0|\mathbf{r}-\mathbf{r}'|}}{|\mathbf{r}-\mathbf{r}'|}d\mathbf{r}' = -\nabla\phi \tag{1}$$

where V is the union of the conductor volumes, $\mathbf{r}$ is a point in V, $\omega = 2\pi f$ is the angular frequency of the conductor excitation, and $k_0 = \omega\sqrt{\mu\varepsilon}$ is the wave number. The scalar potential *on the conductor surface* can be related to the surface charge, ρ, through

$$\frac{1}{4\pi\varepsilon}\int_S \rho(\mathbf{r}_\mathbf{s}')\frac{e^{jk_0|\mathbf{r}_\mathbf{s}-\mathbf{r}_\mathbf{s}'|}}{|\mathbf{r}_\mathbf{s}-\mathbf{r}_\mathbf{s}'|}d\mathbf{r}_\mathbf{s}' = \phi(\mathbf{r}_\mathbf{s}), \tag{2}$$

where S is the union of the conductor surfaces, and $\mathbf{r}_\mathbf{s}$ is a point in S.

Since the charge in the interior of the conductor is zero,

$$\nabla\cdot\mathbf{J}(\mathbf{r}) = 0 \tag{3}$$

for all points r in the *interior* of V. In addition, the current normal to the conductor surface is responsible for the accumulation of surface charge,

$$\hat{\mathbf{n}}\cdot\mathbf{J}(\mathbf{r}_\mathbf{s}) = j\omega\rho(\mathbf{r}_\mathbf{s}) \tag{4}$$

where $\hat{\mathbf{n}}$ is the unit normal at the point $\mathbf{r}_\mathbf{s}$ on S.

Luca Daniel (510-548-5800 dluca@eecs.berkeley.edu), and Alberto Sangiovanni-Vincentelli (510-642-4882 alberto@eecs.berkeley.edu) are with the Dept. of Electrical Eng. and Computer Science, University of California, 94720 Berkeley, CA. Fax: 510-642-2739.

Jacob White (617-253-2543 white@mit.edu), is with the Dept. of Electrical Eng. and Computer Science, Massachusetts Institute of Technology, Bldg 36-817, 02139 Cambridge, MA. Fax: 617-258-5846.

This work was supported by the MARCO Interconnect Focus Center, by the Semiconductor Research Corporation, and by the Hewlett-Packard Company.

To compute accurate conductor current and charge distributions, or terminal input and coupling impedances, it is necessary to solve the system of integro-differential equations given by (1)-(4). One standard numerical procedure for solving (1)-(4) begins with approximating the volume currents and surface charges by a weighted sum of a finite set of basis functions $\mathbf{w}_j$ and v_j as in $\mathbf{J}(\mathbf{r}) \approx \sum_j \mathbf{w}_j(\mathbf{r}) I_j$, and $\rho(\mathbf{r_s}) \approx \sum_m v_m(\mathbf{r_s}) q_m$, where I_j and q_m are the basis function weights. A Galerkin procedure can be used to generate a system of equations for the weights. The procedure is to substitute the previous representations for $\mathbf{J}$ and ρ into equations (1) and (2) and then insist that the equation residuals are orthogonal to the basis functions. The result is a matrix equation of the form

$$\begin{bmatrix} R + j\omega L & 0 \\ 0 & P \end{bmatrix} \begin{bmatrix} I \\ q \end{bmatrix} = \begin{bmatrix} V \\ \phi \end{bmatrix} \tag{5}$$

where I and q are vectors of current and charge basis function weights, respectively. V and ϕ are the vectors generated by inner products of the volume potential or the surface potential gradient with the basis functions. The matrices R, L and P are derived directly from the Galerkin condition and are given by

$$R_{ij} = \frac{1}{\sigma} \int_V \mathbf{w}_i^*(\mathbf{r}) \cdot \mathbf{w}_j(\mathbf{r})\, d\mathbf{r} \tag{6}$$

$$L_{ij} = \frac{\mu}{4\pi} \int_V \int_V \mathbf{w}_i^*(\mathbf{r}) \cdot \mathbf{w}_j(\mathbf{r}') \frac{e^{jk_0|\mathbf{r}-\mathbf{r}'|}}{|\mathbf{r}-\mathbf{r}'|} d\mathbf{r}' d\mathbf{r} \tag{7}$$

$$P_{lm} = \frac{1}{4\pi\varepsilon} \int_S \int_S v_l^*(\mathbf{r_s})\, v_m(\mathbf{r_s'}) \frac{e^{jk_0|\mathbf{r_s}-\mathbf{r_s'}|}}{|\mathbf{r_s}-\mathbf{r_s'}|} d\mathbf{r_s'} d\mathbf{r_s}. \tag{8}$$

When discretizing relatively long and thin conductors, and for low accuracy applications, piecewise-constant basis functions are typically used. The functions are generated by covering the surface of each conductor with *panels*, each of which hold a constant charge density. To model current flow, the interiors of all conductors are divided into a 3-D grid of *filaments*. Each filament carries a constant current density along its length, and this discretization of the interior captures skin and proximity effects. An example is shown in the figure here on the right.

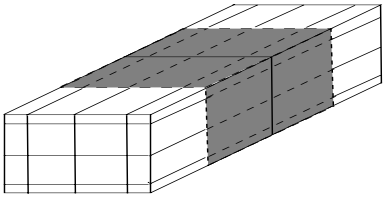

Once the basis functions have been determined and a Galerkin method is used to discretize (1) and (2), then the current conservation conditions in (3) and (4) must be imposed. There are several approaches for imposing these conditions once the discretization has been established [8], [9], [10].

III. Using conduction modes as global basis functions

Using constant density filaments to discretize the current in the interior of the conductors can produce large linear systems at high frequencies. This is because many filaments will be needed to accurately represent the proximity and skin effects. We present in this Section an alternative choice for the volume discretization, where the basis functions are chosen using eigenmodes of an interior Helmholtz equation.

A. Conduction modes

The current inside the conductors satisfies an Helmholtz equation of the form $\nabla \times \nabla \times \mathbf{J} + \left(\frac{1+j}{\delta}\right)^2 \mathbf{J} = 0$, where $\delta = 1/\sqrt{\pi f \mu \sigma}$ is the skin depth, and we have assumed $\sigma \gg j\omega\varepsilon$. Assuming that the current primarily flows in the direction of a conductor length, which we assume to be parallel to the z axis for convenience, the Helmholtz equation simplifies to:

$$\frac{\partial^2 J_z}{\partial x^2} + \frac{\partial^2 J_z}{\partial y^2} - \left(\frac{1+j}{\delta}\right)^2 J_z = 0, \tag{9}$$

where x and y axes align along the width and the thickness of the conductor, respectively.

Solving (9) yields an infinite series representation for the current [11]: $J_z(x,y) = \sum_\nu C_\nu e^{-p_\nu x} e^{-q_\nu y}$, where C_ν's are the "modes" amplitudes and p_ν and q_ν must satisfy the constraint: $p_\nu^2 + q_\nu^2 = \left(\frac{1+j}{\delta}\right)^2$. Boundary conditions and electromagnetic interactions determine the amplitudes of each mode, C_ν.

We have found that a very small number of modes is sufficient to account for the majority of the current distribution. For example, a combination of four simple edge modes, one for each edge, can account for most of the high frequency cross-sectional conductor current distribution. As an illustrative example of a very simple conduction mode, let $p_\nu = (1+j)/\delta$, and $q_\nu = 0$. This mode can account for cross-sectional current distributions decaying exponentially as $1/\delta$ from the edge of the conductor. The second picture from left in Fig. 1 shows a graphical representation of such current distribution.

At very high frequency, few other modes need probably to be added to account for corner effects. The simplest example of corner mode is obtained by choosing: $p_\nu = q_\nu = (1+j)/(\delta\sqrt{2})$. As it is shown in the third picture from left in Fig. 1, this mode can easily account for a cross-sectional current distribution decaying exponentially from the corner of the conductor.

B. Selection of the global basis functions

Assume that any long conductor is first divided into short-length pieces. Then the cross-sectional current densities in each of the pieces can be represented by a collection of global basis functions:

$$\mathbf{J}(\mathbf{r}) = \sum_{j,k} I_{jk} \mathbf{w}_{jk}(\mathbf{r}) \tag{10}$$

where j is a summation index over all the conductor pieces, and k is a summation index over all the global basis functions chosen for each piece. The conduction eigenmodes presented in Section III-A can represent a natural choice for our global basis functions:

$$\mathbf{w}_{jk}(\mathbf{r}) = \begin{cases} \frac{\hat{\mathbf{a}}_{z_j}}{A_{jk}} \sum_v e^{\pm p_{jkv}(x-x_{jkv})} e^{\pm q_{jkv}(y-y_{jkv})} & \text{if } \mathbf{r} \in V_j \\ 0 & \text{otherwise} \end{cases} \tag{11}$$

where x and y are variables spanning the cross-section of conductor piece j, and refer to one of its corners: $\mathbf{r} = \mathbf{r}_{j_{\text{corner}}} + x\hat{\mathbf{a}}_{x_j} + y\hat{\mathbf{a}}_{y_j}$. Translation constants x_{jkv}, y_{jkv}, and "plus" signs in front of p_{jkv} and q_{jkv} account for modes decaying from the other corners or edges. We have chosen to introduce a normalization constant A_{jk} defined such that parameter I_{jk} in eq. (10) represent the part of current on the cross-section associated with basis function $\mathbf{w_{jk}}$: $A_{jk} = \int_{S_j} \sum_v e^{\pm p_{kv}(x-x_{jkv})} e^{\pm q_{kv}(y-y_{jkv})} dx\,dy$.

In eq. (11), we allow to combine several conduction modes into each single basis function, reducing in this way the total number of basis functions. This feature is particularly convenient when modeling for example PCB traces. In this case, one may wish to combine the lower horizontal edge mode with the upper horizontal edge mode into one single basis function as shown in the fourth picture from left in Fig. 1. In fact, the very large aspect ratio of the PCB cross-section traces, and the relative large separation between layers, typically do not allow significant proximity effect differences between lower and upper horizontal edge modes. Large differences, instead, can often be observed between any modes on opposite lateral sides (left to right), due to proximity effects. For this reason, for example the two lateral edge modes should be assigned to two separate basis functions.

C. Discretization of the MPIE

Substituting (10) into (1) and using a Galerkin method we obtain: $\sum_k R_{ihik} I_{ik} + \sum_{j,k} j\omega L_{ihjk} I_{jk} = \phi_A - \phi_B$, where we can recognize terms that could be interpreted as equivalent resistances and partial inductances of the conduction modes basis functions

$$R_{ihik} = \frac{1}{\sigma} \int_{V_i} \mathbf{w}^*_{ih}(\mathbf{r}) \cdot \mathbf{w}_{ik}(\mathbf{r})\, d\mathbf{r} \tag{12}$$

$$L_{ihjk} = \frac{\mu}{4\pi} \int_{V_i} \int_{V_j} \mathbf{w}^*_{ih}(\mathbf{r}) \cdot \mathbf{w}_{ik}(\mathbf{r}) \frac{e^{jk_0|\mathbf{r}-\mathbf{r}'|}}{|\mathbf{r}-\mathbf{r}'|} d\mathbf{r}' d\mathbf{r} \tag{13}$$

With our choice of basis functions, the resistance matrix R is block diagonal. In some cases, e.g. when building Reduced Order Models (ROM), an easily invertible diagonal matrix is more appealing [12], [13]. Such form for R can be recovered by using orthogonalized modes.

IV. Example

We are in the process of implementing our new method into a full-wave electromagnetic interference tool. At this point, we can only give a simple example to show the computational properties of the proposed method. We have implemented code to compute the impedance Z of a typical PCB trace 250μm wide, 35μm thick, and 5mm long. Fig. 2 shows the real part of the impedance ($Re\{Z\}$), and the imaginary part divided by $j\omega$ ($L = Im\{Z\}/j\omega$), as a function of frequency. In this example, we have used a

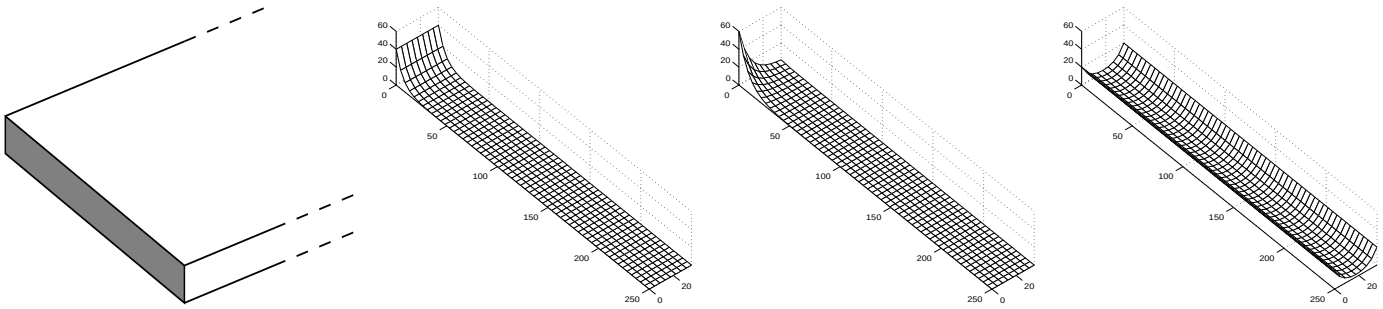

Fig. 1. This figure shows the current modes associated with the shaded cross-section in the picture on the left. Second from left is an "edge mode", then a "corner mode", and fourth from left is a basis function which combines two horizontal edge modes.

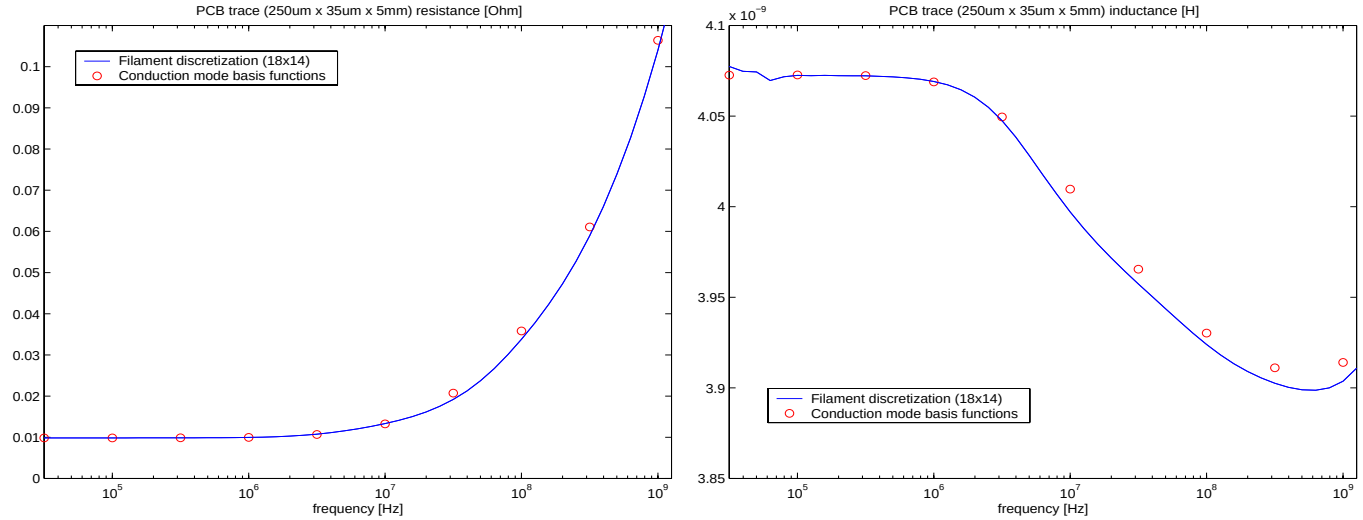

Fig. 2. $Re\{Z\}$ (on the left) and $L = Im\{Z\}/j\omega$ (on the right) vs. frequency for a typical PCB trace. The continuous curves are obtained from a classical very accurate 18x14 filaments discretization approach. Circles indicate results from our new method using, in this particular example, only 3 global basis functions.

classical surface discretization into small panels to account for surface charge, while we have used our conduction-mode global basis functions to account for cross-sectional current density. In particular, we have used the following three basis functions: one for the left side edge-mode (second from left in Fig. 1); one for a similar right edge-mode; and one for the combined upper and lower modes (fourth from left in Fig. 1).

In Fig. 2, we compare our method with one that uses the same discretization into small panels for the surface charge, and a very accurate cross-sectional discretization into 18x14 small filaments for the volume currents. In this filament method, filament thickness is decreased at a ratio of 1.5 at each step as we get closer to the edges. Compared to this accurate filaments approach, our method shows in the worst case: a 5% error in the resistive part of the impedance $Re\{Z\}$, and a very small 0.2% error in the inductive part of the impedance $L = Im\{Z\}/j\omega$.

In a second experiment on the same example, we have observed that, in order to achieve the same errors of our conduction modes method, the filament method requires 10x7 small filaments per cross-section, with thickness decreasing at a ratio of 5 at each step as we get closer to edges and corners. Hence in this example, for the same final accuracy, our method produced a system 20 times smaller than the filament discretization method.

V. Conclusions

In this paper, a new method has been presented for modeling internal conductor current distributions in a quasi-static or full-wave electromagnetic simulator. We have shown how to derive conduction modes, and how to use them as global basis functions for the discretization of the Mixed Potential Integral Equation. Finally, we have presented the potential of our method on a simple example, where linear systems 20 times smaller than the classical filament discretization methods are obtained for the same final accuracy.

References

[1] K. Nabors and J. White. Fastcap: a multipole accelerated 3-d capacitance extraction program. *TCAD*, pages 1447–59, November 1991.

[2] S. Kapur and D. Long. Large scale capacitance calculations with nebula. In *Design Automation Conference*, June 2000.

[3] J. R. Phillips, E. Chiprout, and D. D. Ling. Efficient full-wave electromagnetic analysis via model order reduction of fast integral transforms. In *Design Automation Conference*, June 1996.

[4] J. Tausch and J. White. A multiscale method for fast capacitance extraction. In *Design Automation Conference*, June 1999.

[5] E. Tuncer, B. T. Lee, and D. P. Neikirk. Interconnect series impedance determination using a surface ribbon method. *IEEE Topical Meeting on Electrical Performance of Electronic Packaging*, pages 250–252, November 1994.

[6] K. M. Coperich, A. E. Ruehli, and A. C. Cangellaris. Enhanced skin effect for partial element equivalent circuit (peec) models. In *IEEE Topical Meeting on Electrical Performance of Electronic Packaging*, October 1999.

[7] J. Wang, J. Tausch, and J. White. A wide frequency range surface integral formulation for 3-d rlc extraction. In *IEEE Internat. Conf. on Computer-Aided Design*, pages 456–460, 1997.

[8] A. E. Ruehli. Equivalent circuit models for three dimensional multiconductor systems. *IEEE Trans. on Microwave Theory and Techniques*, 22:216–221, March 1974.

[9] N. Marques, M. Kamon, J. White, and L. M. Silveira. A mixed nodal-mesh formulation for efficient extraction and passive reduced-order modeling of 3d interconnects. In *Design Automation Conference*, pages 297–302, 1998.

[10] M. Kamon, N. Marques, L. M. Silveira, and J. White. Automatic generation of accurate circuit models. *IEEE Trans. on Comp., Packaging, and Manufact. Tech.*, August 1998.

[11] E. M. Deeley. Surface impedance near edges and corners in three-dimensional media. *IEEE Trans. on Magnetics*, 2:712–714, 1990.

[12] A. Odabasioglu, M. Celik, and L. T. Pileggi. Prima: Passive reduced-order interconnect macromodeling algorithm. *IEEE Trans. on Computer-Aided Design of Integrated Circuits and Systems*, pages 645–654, August 1998.

[13] L. M. Silveira, I Elfadel, M. Kamon, and J. White. Coordinate-transformed arnoldi algorithm for generating guarantee stable reduced-order models of rlc. *Special Issue on Advances of Comp. Methods in Electromagnetics*, pages 377–389, February 1999.